INSTITUTE OF PHYSICS PUBLISHING JOURNAL OF PHYSICS B: ATOMIC, MOLECULAR AND OPTICAL PHYSICS

J. Phys. B: At. Mol. Opt. Phys. **37** (2004) 1951–1960 PII: S0953-4075(04)74564-2

Cascades between doubly excited levels in helium-like argon

O Marchuk[1], G Bertschinger[1], H-J Kunze[2], N R Badnell[3] and S Fritzsche[4]

[1] Institut für Plasmaphysik, Forschungszentrum Jülich, D-52425, Germany
[2] Institut für Experimentalphysik V, Ruhr-Universität Bochum, Bochum, Germany
[3] Department of Physics, University of Strathclyde, Glasgow G4 0NG, UK
[4] Department of Physics, University of Kassel, Kassel, D-34109, Germany

Received 8 January 2004
Published 23 April 2004
Online at stacks.iop.org/JPhysB/37/1951 (DOI: 10.1088/0953-4075/37/9/014)

Abstract

Helium-like spectra produced by photon emission of ions with intermediate Z represent an important diagnostic for fusion plasmas and solar flares. In this work, the influence of the radiative transitions among doubly excited levels on the intensity of the associated dielectronic satellites ($1s^2nl$–$1s2lnl'$) is analysed. Special attention is paid to the comparison between inner-shell excited satellites of $n = 2$ and different theoretical calculations. We described the group of $n = 3$ and $n = 4$ dielectronic satellites taking into account additional radiative channels to the group of $n = 2$. Cascade contributions have been verified in experimental spectra of argon from the tokamak TEXTOR. We have compared the intensity of all resolved satellites of $n = 2$ and the group of $n = 3$ with experiment. The internal consistency for the satellites with and without inner-shell excitation part has been achieved. Most important is the effect on the measurement of lithium-like ions, determined from the collisional satellites. The measured concentrations prove the prediction of transport simulation, taking into account the diffusion of ions and charge exchange recombination. The strong satellites of $n = 2$, providing the results on electron temperature, are found to be not sensitive to the cascades.

1. Introduction

Helium-like spectra emitted from high temperature plasmas and solar flares provide information on plasma parameters, such as ion and electron temperature or the distribution of highly ionized ions. Helium-like species exist in a broad temperature range and this suggests the application of the spectra to the diagnostic of fusion and laser produced plasma [1, 2]. Such measurements have been previously done at the Princeton Large Torus Experiment (PLT), at TFTR, at the Tokamak Fontenay aux Roses (TFR) and at the Alto Campo Torus (ALCATOR). Nowadays research on the helium-like system is carried out at the tokamaks TORE SUPRA,

TEXTOR, ALCATOR-C(mod), JET-EFDA, LHD and NSTX. The new generation of space satellites will also utilize the same technique for the investigation of solar flares [3].

The first theoretical description of the satellite spectra was performed by Gabriel [4] on the basis of solar flares. Additional attempts to describe the satellite spectra were made by Vainshtein on the basis of helium-like iron [5]. The photon statistics was unfortunately too poor to investigate the spectra in detail. X-ray spectrometers installed at a number of fusion machines such as JET, LHD, NSTX and TEXTOR allow us now to obtain the spectra with much higher quality. The stationary plasma operation ensures a high photon statistical level of the experiment at the low density limit. The setup of most spectrometers is designed to provide a maximum of spectral resolution [6], comparable now with theoretical calculations [7]. The helium-like spectra from fusion devices including EBIT sources [8] are, therefore, well qualified for the verification of atomic data in systems with few electrons. This research includes modelling of dielectronic satellites, excitation processes of helium-like target and precise energy calculations. The development of the atomic theory for the description of the dielectronic satellites has been performed for helium-like spectra for elements with intermediate Z such as calcium and iron [9, 10].

The theoretical description of the spectra is not possible without taking into account the dielectronic satellite structure. Dielectronic recombination, the process by which an atomic ion captures a free electron into a doubly excited state and subsequently decays by spontaneously emitting a photon, is an important cooling mechanism in hot plasmas. The high-resolution instruments allow us now to distinguish satellites of the transition $1s^2 2l$–$1s2l2l'$ in the spectra and the group of transitions $1s^2 nl$–$1s2lnl'$. Simultaneous measurements of the group of $n = 3$ dielectronic satellites and of different $n = 2$ satellites can be used for the verification of different atomic approaches to the description of the satellites.

The perturbative theory method is the basis of the MZ code developed by Vainshtein and Safronova for calculating the energy of the satellites and the radiative and the autoionization rates [11]. This method uses the Z-expansion for atomic parameter calculations. The energy matrix constructed in LS-coupling includes relativistic and non-relativistic parts. The non-relativistic part takes into account three terms of the Z-expansion. The relativistic part is constructed using the Breit–Pauli operator. The inconsistency of the method for satellites belonging to $n = 2$ and $n = 3$ was proved experimentally and reported in [12]. The other approach, introduced in the SUPERSTRUCTURE program developed by Eisner *et al* [13], involves the diagonalization of the Hamiltonian on the set of basis configurations. The calculations presented in this paper are based on the AUTOSTRUCTURE program, the extended version of SUPERSTRUCTURE developed by Badnell [14]. Slater-type orbital potentials are used for finding the wavefunctions. Moreover, the recent partial cross section calculations of the dielectronic recombination provided by the eigenchannel R-matrix approach based on the close-coupling technique, and AUTOSTRUCTURE proved agreement for lithium-like argon [15]. To calculate the transition strengths between the doubly excited states, we also applied multi-configuration Dirac–Fock (MCDF) wavefunctions as generated by means of the GRASP [16] and RATIP programs [17]. In these computations, an atomic state is approximated by a linear combination of configuration state functions as obtained from a proper distribution of the two respectively three electrons among the subshells. In standard computations, the configuration states are antisymmetrized products of a common set of orthonormal orbitals which are optimized on the basis of the Dirac–Coulomb Hamiltonian. Further relativistic corrections due to the (transverse) Breit interaction have been added as well but are found to be rather small for argon.

With increasing accuracy of the theoretical data, it is now possible to model the spectra with physically relevant parameters only, such as electron and ion temperature, plasma motion and

relative abundance of the different ionization stages. Accurate values of the dielectronic part of the collisional satellites are required for the measurement of the lithium-like concentration. The obtained values control the impurity transport modelling in tokamaks and solar flares. In addition to this, the deviation from the ionization balance as a function of plasma parameters can be carefully studied.

Up to now, the influence of the cascades between doubly excited states of the lithium-like system on the intensity of the satellites has been neglected in all previous calculations. In the first section we consider the intensity of the dielectronic satellites and their enhancement due to additional population channels, especially for the $n = 2$ satellites. In the next section, we compare experimental spectra recorded on the tokamak TEXTOR to our theoretical simulations.

2. Cascade effects between doubly excited states of lithium-like ions

The satellite lines are one of the most important source of plasma information. The intensity of any lithium-like satellite due to dielectronic capture is given by

$$I_s(i, j) = N_{He} N_e \frac{4\pi^{3/2} a_0^3}{T_e^{3/2}} \frac{g_s}{g_0} \frac{A_r(i, j) \cdot A_a(i)}{\sum_{l<i} A_r(i, l) + A_a(i)} \exp\left(-\frac{E_s}{T_e}\right), \tag{1}$$

where i is the initial level of satellites belonging to one of the doubly excited states of lithium-like ions; j is the final level of the satellites; N_{He}, N_e are the density of helium-like ions and electron density, respectively; g_s, g_0 are the statistical weights of the initial level i of the dielectronic satellite and the ground state of helium-like ion; a_0 is the Bohr radius; $A_r(i, j)$, $A_a(i)$ are the radiative rate from level i to j and autoionization rate from level i in $1/s$, correspondingly; E_s is the excitation energy of a satellite above the helium-like ground state, in Ryd; T_e is the electron temperature in Ryd. Dubau [18] introduced F_2-values to separate the atomic properties from the temperature-dependent parts:

$$F_2(i, j) = \frac{g_s \cdot A_a(i) \cdot A_r(i, j)}{\sum_{l<i} A_r(i, l) + A_a(i)}. \tag{2}$$

In addition to this source of population by dielectronic capture, we have considered the process of radiative decay among doubly excited levels in lithium-like ions, as shown in figure 1.

As the temperature dependence is the same for all satellites the initial population of the doubly excited states obeys the relation:

$$N(i) \sim g_s A_a \exp\left(-\frac{E_s}{T_e}\right) \tag{3}$$

Since the autoionization rates scale as $1/n^3$ for different groups of dielectronic satellites, we restricted our considerations only up to $n = 5$ in intermediate coupling. Although radiative transitions to the ground state dominate, the transitions among doubly excited states become important for the levels with low autoionization. The initial population in these levels (3) is comparable in this case with the contribution by cascades. The intensity of the satellites can, therefore, be expressed as

$$I_s(i, j) = N_{He} N_e \frac{4\pi^{3/2} a_0^3}{T_e^{3/2}} \cdot \frac{F_2(i, j)}{g_0} \cdot \gamma(i, T_e) \cdot \exp\left(-\frac{E_s}{T_e}\right), \tag{4}$$

where $\gamma(i, T_e)$ is a correction function to the satellite intensity through the cascades.

The influence of the cascades increases with the temperature as in the excitation processes. Therefore, we obtain the maximum of the additional contribution in the limit of infinite

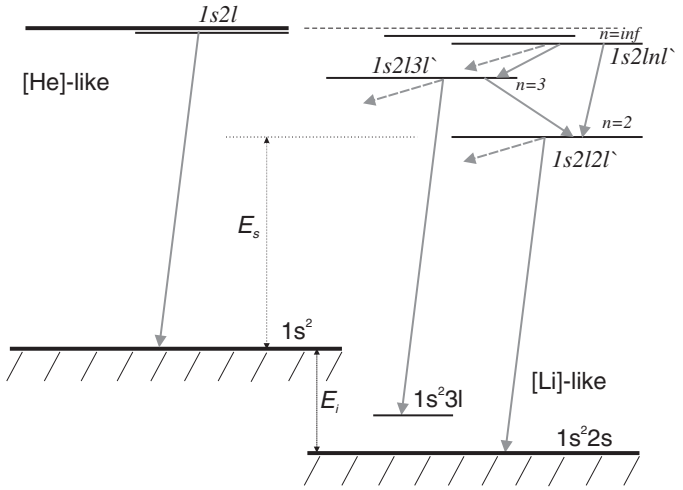

Figure 1. Energy level diagram of helium- and lithium-like ions.

Table 1. Values of radiative and autoionization rates and F_2-values in 10^{13} s^{-1}. The correction γ is presented at an electron temperature of 0.5, 2.0, 4.0 keV. The last column gives the maximum values of γ at infinite temperature.

Key	Transition	A_r	A_a	F_2	$\gamma(0.5)$	$\gamma(1.0)$	$\gamma(2.0)$	$\gamma(4.0)$	γ_{max}
s	$1s^22s(^2S_{1/2})$–$1s2p2s(^3P)(^2P_{3/2})$	0.69	9.76	2.57	1.02	1.03	1.04	1.04	1.05
t	$1s^22s(^2S_{1/2})$–$1s2p2s(^3P)(^2P_{1/2})$	2.34	8.50	3.67	1.01	1.02	1.03	1.04	1.04
q	$1s^22s(^2S_{1/2})$–$1s2p2s(^1P)(^2P_{3/2})$	9.91	0.33	1.25	1.5	1.84	2.10	2.26	2.45
r	$1s^22s(^2S_{1/2})$–$1s2p2s(^1P)(^2P_{1/2})$	8.29	1.60	2.68	1.10	1.17	1.23	1.26	1.30
a	$1s^22p(^2P_{1/2})$–$1s2p^2(^2P_{3/2})$	14.1	0.95	3.31	1.01	1.02	1.02	1.02	1.03
k	$1s^22p(^2P_{1/2})$–$1s2p^2(^2D_{3/2})$	5.86	14.7	16.7	1.01	1.01	1.01	1.01	1.01
j	$1s^22p(^2P_{3/2})$–$1s2p^2(^2D_{5/2})$	5.11	15.4	23.0	1.01	1.01	1.01	1.01	1.01

temperature. On the other hand, taking into account cascade processes decreases the intensity of the high-n satellites and diminishes the discrepancy between theoretical simulations and experimental results reported in [19]. Strictly speaking, the values of $\gamma(i, T_e)$ depend not only on the electron temperature and autoionization of the level i, but also on how many states have been considered in the cascade matrix. We restricted ourselves up to $n = 5$, as the population from higher n contributes less than 5% of the total contribution. The cascades from the states with $n = 3$ dominate, as expected.

In table 1 we present the results of our calculations for the most prominent satellites belonging to the group with $n = 2$. In addition to F_2-values, autoionization and radiative rates we show the values of the function γ at different electron temperatures.

Special attention was paid to the group of $n = 2$ dielectronic satellites of the configuration 1s2p2s (**s**, **t**, **q** and **r** lines). The initial population of the levels from this configuration is relatively small in comparison with the other levels of the groups $n = 3$ and $n = 4$. A strong inner-shell excited part of this configuration suggests the use of this group of satellites for the measurement of the lithium-like abundance.

The calculations were as follows: level energies, autoionization and radiative rates were obtained using the AUTOSTRUCTURE program. The collisional-radiative modelling has been applied to the transitions to calculate the cascades between doubly excited levels. The

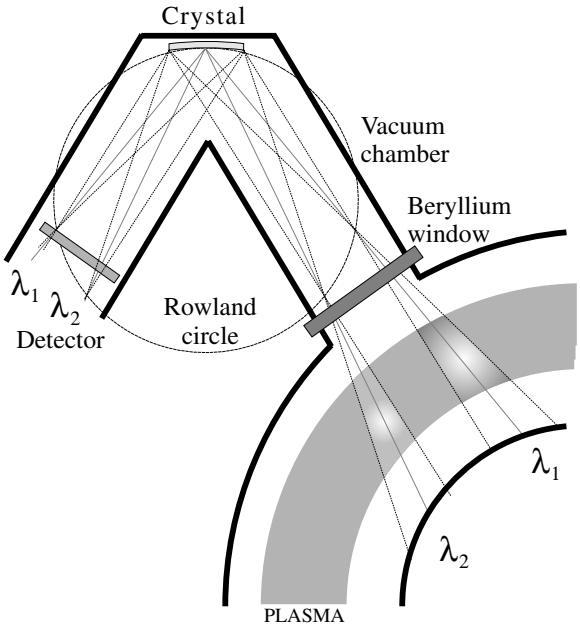

Figure 2. Overview of x-ray spectrometer on the tokamak TEXTOR.

initial population on the doubly excited states was taken according to equation (3), and then the population through the cascades was calculated as a function of temperature. The obtained results were transferred finally to the correction function γ. The importance of the cascades had been first observed using radiative rates calculated by the MCDF method. In these computations, the configuration basis has been increased systematically to incorporate all the singly and doubly excited states from the $1s2lnl'$ configurations with $n \leqslant 5$. Both radiative and Auger transition probabilities have then been calculated by means of the components of the RATIP package [17]. For the dipole moments, various approaches agree to within 20% for most of the transitions between levels of the group with $n = 4$, $n = 3$ and $n = 2$. The radiative rates to the ground states from $n = 2$ differ by a few per cent. Unfortunately the values of the autoionization rates for the $n = 2$ satellites obtained from RATIP do not agree with new and previous calculations [11].

3. Experimental setup

The spectra have been measured on the tokamak TEXTOR. The experimental setup of the spectrometer is shown in figure 2. The typical operational conditions of a tokamak, electron density 2–10 $\times$ 10^{13} cm^{-3} and electron temperature above 1 keV, allow us to describe all the atomic processes in the low density (coronal) limit. The ions are in the ground states of the respective ionization stages, and excited states decay spontaneously, either by radiative decay or by autoionization. For the highly charged ions with $Z > 10$ this is valid even for the long living metastable state $1s2s(^1S_0)$, where the two-photon decay to the ground state is more frequent than de-excitation by collisions with electrons. The temperature range of 1.0 to 2.5 keV in which the helium-like argon is the most abundant ionization stage in the plasma core provides ideal conditions for the examination of the quality of the atomic data and, at the same time, for obtaining plasma parameters. Measurements of ion and electron temperature as

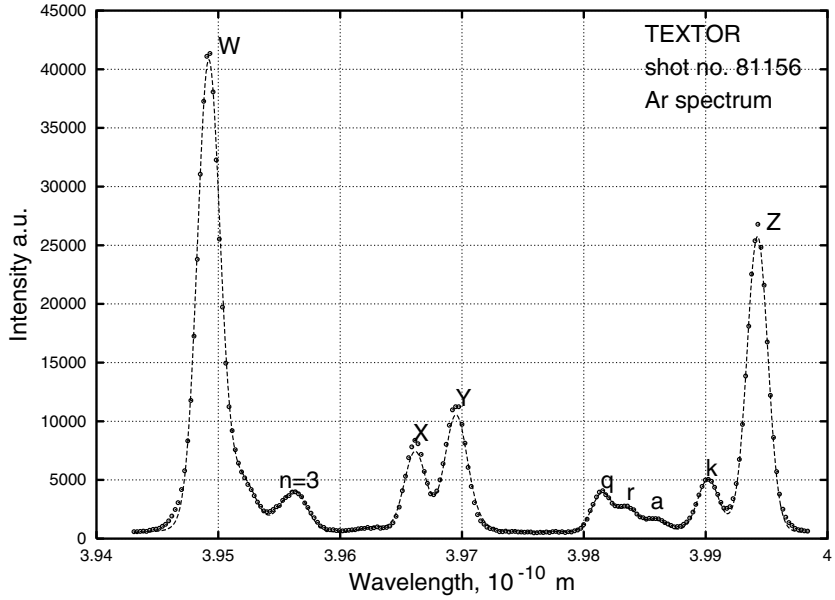

Figure 3. Experimental helium-like spectrum of argon from tokamak TEXTOR. Open points: experimental spectrum, dashed line: theoretical simulation including cascades between doubly excited levels.

well as toroidal plasma velocity and high-charge state abundances are the features of this kind of diagnostics at TEXTOR. The Johann–Bragg spectrometer installed at TEXTOR [20] uses a cylindrically bent quartz crystal as the dispersion element and a multi wire proportional counter (MWPC) for the measurement of emitted photons from the plasma. Due to the properties of the Bragg reflection, no entrance slit is necessary and the whole spectrum is focused on the detector.

The Bragg angle of the instrument is about 54°. An absolute calibration is not required due to the narrow spectral range of the spectrometer, 3.94–4.05 Å. High spectral resolution of the instrument $\Delta\lambda/\lambda$, which exceeds 5000, allows us to distinguish the discrete helium-like lines and separate satellites belonging to the group of $n = 2$. The resonance line of the helium-like system is adjusted at the focus position on the Rowland circle. The instrumental function consists of Gaussian and Lorentzian parts and is used to describe the broadening of the lines at different positions on the MWPC [20].

4. Comparison with experiment

A spectrum of helium-like argon is presented in figure 3. The lines, following Gabriel's notation [4] are the resonance line **w**: $1s^2(^1S^0)$–$1s2p(^1P_1)$, the intercombination line **y**: $1s^2(^1S^0)$–$1s2p(^3P_1)$ and the forbidden lines **x**: $1s^2(^1S^0)$–$1s2p(^3P_2)$ and **z**: $1s^2(^1S^0)$–$1s2s(^3S_1)$. These lines are produced mainly by direct collisional excitation from the helium-like ground state with contributions by cascades from higher levels in the helium-like system. *R*-matrix calculations [21] have been taken for the excitation rates in our modelling.

Inner-shell ionization of the configuration $1s^22s$ contributes to the intensity of the **z** line. The strength of this contribution depends on the lithium-like abundance in the plasma. Recombination consisting of dielectronic and radiative components enhances the intensity of

the helium-like lines at higher temperatures. Charge exchange recombination contributes to the line intensities with the presence of neutrals in the plasma.

The satellites present in the spectrum are due to transitions $1s^2nl$–$1s2lnl'$ with $n \geqslant 2$ in the doubly excited lithium-like system. The doubly excited levels are either populated by dielectronic recombination or by collisional inner-shell excitation. The most intense satellites are **k**: $1s^22p(^2P_{1/2})$–$1s2p^2(^2D_{3/2})$, **j**: $1s^22p(^2P_{3/2})$–$1s2p^2(^2D_{5/2})$, **q**: $1s^22s(^2S_{1/2})$–$1s2p2s(^1P)(^2P_{3/2})$, **r**: $1s^22s(^2S_{1/2})$–$1s2p2s(^1P)(^2P_{1/2})$, **s**: $1s^22s(^2S_{1/2})$–$1s2p2s(^3P)(^2P_{3/2})$, **t**: $1s^22s(^2S_{1/2})$–$1s2p2s(^3P)(^2P_{1/2})$. The satellites with higher n could not be resolved in the spectrum because of Doppler broadening. However, these lines change the shape of the **w** line in the spectrum.

The effect of cascade contributions to the satellite intensity is most pronounced for the $n = 2$ dielectronic satellites with low autoionization rates. It turns out that the configuration 1s2s2p is mostly affected by the additional population channels. The intensity of the **q** and **r** satellites considerably increases due to cascade effects as a function of temperature. The satellites **s** and **t** blend with the **x** and **y** lines in the spectrum and they cannot be clearly distinguished from these lines in the plasma with a Maxwell distribution of the electrons. It is possible to avoid this blend in EBIT experiments, with a slow energy ramp of the electron beam [22], where the different processes can be classified according to the electron energy. The cascade contribution for **s** and **t** satellites is negligible (table 1). The satellites **q** and **r** have a strong inner-shell excitation part and are used to measure the density of the lithium-like ions. The inner-shell excitation rates for the collisional part of the satellites have been taken from R-matrix calculations. The effective rate coefficients are in agreement to within 5% with the calculations by Dubau for iron and titanium [10, 23].

The effect of the cascades on the measurement of the concentration of Li-like ions is most important at intermediate plasma temperature. At high temperature the collisional part of the satellites **q** and **r** and of the resonance line **w** rises significantly faster than the dielectronic contributions to the lines including cascades. At low temperatures the density of lithium-like ions starts to increase through the recombination processes of the helium-like ions. It leads to an increase of the collisional part of the **q** and **r** satellites as well. Therefore, we have compared the theoretical predictions and experimental values at temperatures $T_e = 1.0$–1.1 keV, when the dielectronic part is comparable to the inner-shell excitation and the helium-like abundance is much higher than lithium-like one. Even though x-ray spectroscopy is a diagnostic for the hot plasma core, precise modelling of the spectra requires integration along the line of sight, as the concentrations of ions in the different ionization stages vary with the plasma radius. The radial profiles of highly ionized charge state distribution have been taken from transport code calculations, electron density and temperature profiles have been taken from the HCN interferometer and the emission at the cyclotron emission frequency (ECE); the electron temperature profile has been normalized to the result of the spectra simulation. The diffusion coefficients used in the transport modelling have been determined experimentally from the gas puff experiments [24].

For the intensities of dielectronic satellites we used new calculations made by AUTOSTRUCTURE with and without cascades and data obtained by Vainshtein and Safronova [11, 25] and by Dubau [26]. The electron temperature was obtained from the ratio of the well-separated **k** satellite and the **w** line. The theoretical intensity of the **k** satellite, i.e the F_2-value, obtained by the different calculations, does not differ by more than 7%.

The comparison between the experimental spectra and atomic data shows (figure 4) a relatively good description of the group of the **q**, **r** and **a** satellites by all approaches. Nevertheless, the present results show better agreement for the description of the **a** satellite. The approach used by Safronova and Vainshtein predicts, in contrast to this, precise

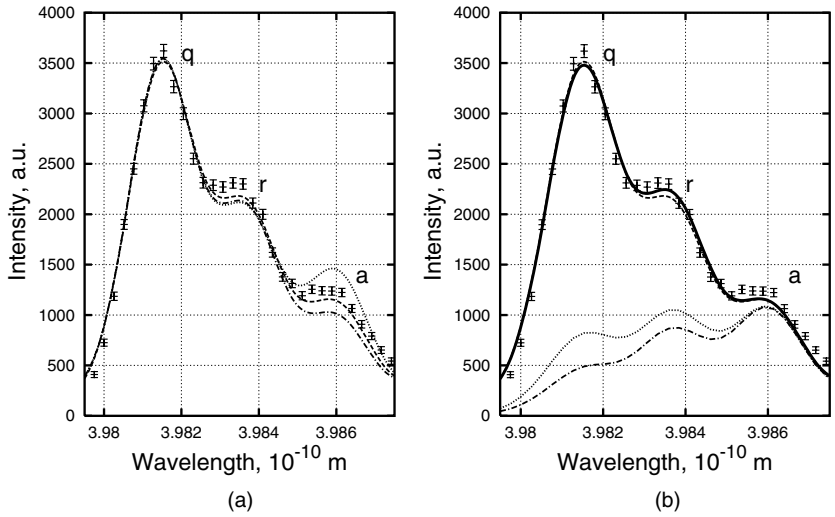

Figure 4. Experimental and theoretical spectra: **q**, **r** and **a** satellites. Shot 81156, TEXTOR. $t = 0.8$–3.9s, $T_e = 1.05$–1.1 keV. (a) Error bars: experimental spectra, dashed line: present calculations without cascades, dotted line: calculations by Vainshtein, Safronova [11], dashed-dotted line: calculations by Cornille, Dubau [26]. (b) Error bars: experimental spectra, solid line: present calculations with cascades, dashed line: without cascades, dotted line: dielectronic satellites with cascades, dashed-dotted line: dielectronic satellites without cascades.

wavelengths for the helium- and lithium-like systems. Their calculations are also found to be in good agreement with EBIT measurements [8] or precision calculations by Plante and Johnson for the $n = 2$ levels in the helium-like sequence [7].

The increase of the intensity of the **a** satellite through cascades, as seen from table 1, is negligible. This is confirmed by our experiment. The cascades change the ratio of the dielectronic part of the lines **q** and **r**, although it is compensated by a decrease of the collisional parts of the lines.

The most important effect of cascades is seen on the measurements of lithium-like argon. The increased dielectronic part of the **q** and **r** satellite diminishes the concentration of the lithium-like ions in the system. The density changes by 10–25% with respect to values without cascades. This behaviour is presented in figure 5, where the measured concentration versus electron density is shown. The absolute difference of the measured lithium-like concentration with and without cascades is approximately the same in the density interval of 1×10^{13}–5×10^{13} (cm^{-3}). The obtained abundance of the lithium-like ions coincides with the transport modelling in the core [24]. The cascades have no influence on the measurements of the electron temperature as the theoretical ratio between the satellites **k** and **w** did not change (table 1). The measurements of the electron temperature from other spectra such as from iron or titanium remain constant as well. In these spectra the ratio of the **j** line and the **w** line is used for the measurements of the electron temperature.

An additional decrease of the higher n satellites has been seen in the spectra description. The cascades decrease the intensity of the groups of the $n = 3$ and $n = 4$ dielectronic satellites by up to 5%. The measurement of the electron temperature based on this group of satellites is discussed by Bitter [19]. These measurements of electron temperature from $n = 2$ and $n = 3$ have also pointed to the overestimated satellite intensities for $n = 3$ in the MZ calculations.

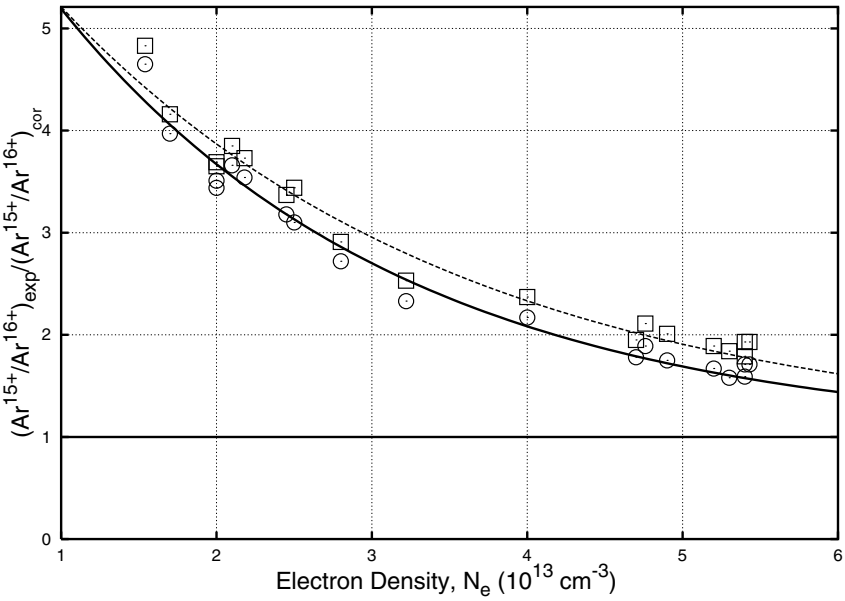

Figure 5. Ratio of measured lithium-like concentration divided by the coronal value. Open squares: measurements without cascades, open circles: with cascades. The dashed curves indicate the behaviour of the ratio.

5. Conclusions

The new calculations using the AUTOSTRUCTURE program for lithium-like dielectronic satellites have been used to reproduce the experimental spectra from the tokamak TEXTOR. The obtained atomic data have been found to be in good agreement with previous calculations.

The cascades among doubly excited levels have now been carefully studied in the low density limit. They affect the intensity of dielectronic satellites having low autoionization rates. The population of the upper levels of the satellites, having a strong inner-shell excited part, increased considerably (**q** and **r** lines). This influences the measurements of the abundance of lithium-like ions. The density of the ions decreases by 10–25% in the temperature interval between 0.8 and 2.0 keV. At higher temperatures the contribution of the inner-shell excitations starts to dominate the dielectronic part of the lines. The measurements are important for the understanding of the transport properties and neutral penetration to the plasma, as x-ray spectroscopy is the only diagnostic providing the charge stage distribution of the hot plasma core. The obtained results have verified the transport coefficients and the ionization stage distribution in the plasma. The measurements of electron temperature by strong dielectronic satellites such as **j** and **k** have no dependence on the transitions among doubly excited states.

In high density plasmas, the dielectronic satellites should be described in the frame of a full kinetic model. It includes in addition to the radiative decay considered in this paper collisional redistribution of autoionizing states. In this high density regime the intensity of the lines **q** and **r** can then be used for the determination of the plasma density [27]. The low density fusion plasma does not require such modelling as radiative decay occurs before electron and heavy particle collisions can take place.

References

[1] Bombarda F, Gianelli R, Källne E, Tallents G J, Bely-Dubau F, Faucher P, Cornille M, Dubau J and Gabriel A H 1988 *Phys. Rev.* A **37** 504
[2] Gabriel A H and Paget T M 1972 *J. Phys. B: At. Mol. Phys.* **5** 673
[3] Philips K J H, Harra L K, Keenan F P, Zarro D M and Wilson M 1993 *Astrophys. J.* **419** 426
[4] Gabriel A H 1972 *Mon. Not. R. Astron. Soc.* **160** 99
[5] Grineva Yu I, Karev V I, Korneev V V, Krutov V V, Mandelstam S L, Vainshtein L A, Vasilyev B N and Zhitnik I A 1973 *Solar Phys.* **23** 441
[6] Platz P, Cornille M and Dubau J 1996 *J. Phys. B: At. Mol. Opt. Phys.* **29** 3787
[7] Johnson W R, Plante D R and Sapirstein J 1995 *Adv. At. Mol. Opt. Phys.* **35** 255
[8] Tarbutt M R, Barnsley R, Peacock N J and Silver J D 2001 *J. Phys. B: At. Mol. Opt. Phys.* **34** 3979
[9] Bely-Dubau F, Dubau J, Faucher P, Gabriel A H, Loulergue M, Steenman-Clark L, Volonte S, Antonucci E and Rapley C G 1982 *Mon. Not. R. Astron. Soc.* **201** 1155
[10] Bely-Dubau F, Dubau J, Faucher P and Gabriel A H 1982 *Mon. Not. R. Astron. Soc.* **198** 239
[11] Vainshtein L A and Safronova U I 1978 *At. Data Nucl. Data Tables* **21** 44
[12] Bertschinger G, Biel W, Herzog O, Weinheimer J and Kunze H-J 1999 *Phys. Scr.* T **83** 132
[13] Eissner W, Jones M and Nussbaumer H 1974 *Comput. Phys. Commun.* **8** 270
[14] Badnell N R 1997 *J. Phys. B: At. Mol. Opt. Phys.* **30** 1
[15] Gorczyca T W, Robicheaux F, Pindzola M S and Badnell N R 1996 *Phys. Rev.* A **54** 2107
[16] Parpia F A, Froese Fischer C and Grant I P 1996 *Comput. Phys. Commun.* **94** 249
[17] Fritzsche S 2001 *J. Electron Spectrosc. Relat. Phenom.* **114** 1155
[18] Bely-Dubau F, Gabriel A H and Volonte S 1979 *Mon. Not. R. Astron. Soc.* **186** 405
[19] Bitter M *et al* 2003 *Phys. Rev. Lett.* **91** 265001
[20] Weinheimer J, Ahmad I, Herzog O, Kunze H-J, Bertschinger G, Biel W, Borchert G and Bitter M 2001 *Rev. Sci. Instrum.* **72** 2566
[21] Whiteford A D, Badnell N R, Ballance C P, O'Mulane M G, Summers H P and Thomas A L 2001 *J. Phys B: At. Mol. Opt. Phys.* **34** 3179
[22] Biedermann C, Radtke R and Fussman G 1997 *Phys. Rev.* A **56** R2522
[23] Bely-Dubau F, Faucher P, Steenman-Clark L, Bitter M, von Goeler S, Hill K W, Camhy-Val C and Dubau J 1982 *Phys. Rev.* A **26** 6
[24] Biel W 2001 *Proc. 28th European Conf. on Controlled Fusion and Plasma Physics, Europhysics Conference Abstracts, ECA* vol 25A p 1389
[25] Vainshtein L A and Safronova U I 1980 *At. Data Nucl. Data Tables* **25** 311
[26] Bombarda F, Bely-Dubau F, Faucher P, Cornille M, Dubau J and Loulergue M 1985 *Phys. Rev.* A **32** 2374
[27] Antsiferov P S, Rosmej F B, Rosmej O N, Schmidt H, Schulz D and Schulz A 1995 *J. Appl. Phys.* **77** 4973